Optics Communications 289 (2013) 123–126

Contents lists available at SciVerse ScienceDirect

Optics Communications

journal homepage: www.elsevier.com/locate/optcom

An all-photonic-crystal-fiber wavelength-tunable source of high-energy sub-100 fs pulses

Xiao-Hui Fang [a], Ming-Lie Hu [a], Bo-Wen Liu [a], Lu Chai [a], Ching-Yue Wang [a], Hui-Feng Wei [b], Wei-Jun Tong [b], Jie Luo [b], Chi-Kuang Sun [c], Alexander A. Voronin [d,e], Aleksei M. Zheltikov [d,e,f,*]

[a] Ultrafast Laser Laboratory, Key Laboratory of Opto-electronic Information Science and Technology of Ministry of Education, College of Precision Instruments and Opto-electronics Engineering, Tianjin University, Tianjin, 300072, China
[b] Yangtze Optical Fiber and Cable Company Ltd., Wuhan 430073, China
[c] Department of Electrical Engineering, National Taiwan University, Taipei 10617, Taiwan
[d] Physics Department, International Laser Center, M.V. Lomonosov Moscow State University, 119992 Moscow, Russia
[e] Russian Quantum Center, ul. Novaya 100, Skolkovo, Moscow Region, 1430125, Russia
[f] Department of Physics and Astronomy, Texas A&M University, 77843 College Station TX, USA

ARTICLE INFO

Article history:
Received 22 January 2011
Received in revised form
19 July 2012
Accepted 21 July 2012
Available online 28 August 2012

Keywords:
Ultrashort pulses
Photonic-crystal fibers
Fiber lasers

ABSTRACT

We demonstrate a wavelength-tunable source of high-energy sub-100 fs light pulses where all the key components, including a master oscillator, an amplifier, and a tunable frequency shifter, are based on photonic-crystal fibers (PCFs). Soliton self-frequency shift in a specifically designed all-solid photonic band-gap fiber with an effective mode area of 110 μm^2 is used in this system to transform a 1040 nm, 50 MHz, 100 fs amplified output of a large-mode-area ytterbium-doped PCF oscillator–amplifier system into sub-100 fs, 6.4 nJ light pulses smoothly tunable within the range of wavelengths from 1160 to 1260 nm.

Photonic-crystal fibers (PCFs) [1] offer new solutions helping to confront long-standing challenges in fiber-laser technologies. With an appropriate structure design, these fibers can support single-mode guidance for light beams with unprecedentedly large mode areas [1,2]. Such large-mode-area (LMA) PCFs find growing applications in high-energy fiber laser oscillators and amplifiers, including fiber laser sources of ultrashort light pulses [3–8]. LMA PCFs have been also shown to enable the generation of high-energy supercontinuum [9] and high-peak-power solitons [10], as well as to allow compression of a megawatt short-pulse thin-disk [11], fiber-laser [12], and fiber-amplifier [13] output with no degradation of beam quality.

Development of fiber sources of high-contrast ultrashort light pulses, however, requires a careful control over the dispersion profile of fiber components. Such a control is attained with small-core PCFs, where the waveguide dispersion is tailored to balance material dispersion for a targeted dispersion profile within a broad frequency range. In silica-air, "holey" LMA PCF, this strategy of dispersion control is much less efficient, as the dispersion profile in such fibers is typically dominated by material dispersion. All-solid PCFs, also referred to as all-solid photonic band-gap fibers (PBGFs) [14], in many ways help to resolve this difficulty. In PCFs of this class, the light is guided along a silica core by antiresonance reflection from a periodic (photonic-crystal) array of high-index strands in the fiber cladding. As a result, within a limited frequency band of antiresonance reflection, dispersion tailoring for such a fiber can be decoupled from mode-area engineering. All-solid PBGFs have been shown to offer attractive solutions for the generation of ultrashort pulses in mode-locked ytterbium-doped fiber lasers [15], spectral broadening [16,17], as well as for the compression of high-peak-power ultrashort laser pulses [18].

In this work, we use a homemade all-solid PBGF (Fig. 1a and b) with an effective mode area of about 110 μm^2, a waveguide loss of 5 dB/km at 850 nm (solid line in Fig. 2), and a dispersion profile (dashed line in Fig. 2) designed to support soliton propagation within the range of wavelengths from approximately 1060–1400 nm to demonstrate a wavelength-tunable source of high-energy sub-100 fs light pulses. All the key components of this source, such as a master oscillator, an amplifier, and a tunable frequency shifter, are based on PCFs, with the all-solid PBGF serving to transform a 1040 nm, 50 MHz, 100 fs amplified output of a large-mode-area ytterbium-doped PCF oscillator – amplifier

* Corresponding author at: Physics Department, International Laser Center, M.V. Lomonosov Moscow State University, 119992 Moscow, Russia.
Tel.: +7 95 939 5174; fax: +7 95 939 3113.
E-mail address: zheltikov@phys.msu.ru (A.M. Zheltikov).

0030-4018/$ - see front matter © 2012 Published by Elsevier B.V.
http://dx.doi.org/10.1016/j.optcom.2012.07.089

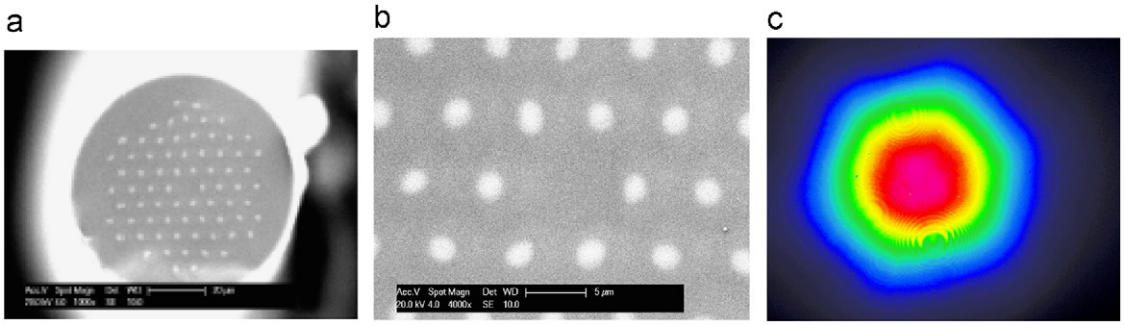

Fig. 1. Electron-microscope images of the fiber cross section (a and b) and an image of the 1040 nm laser beam transmitted through the all-solid PBGF (c). The scale bar in panel (b) is 5 μm.

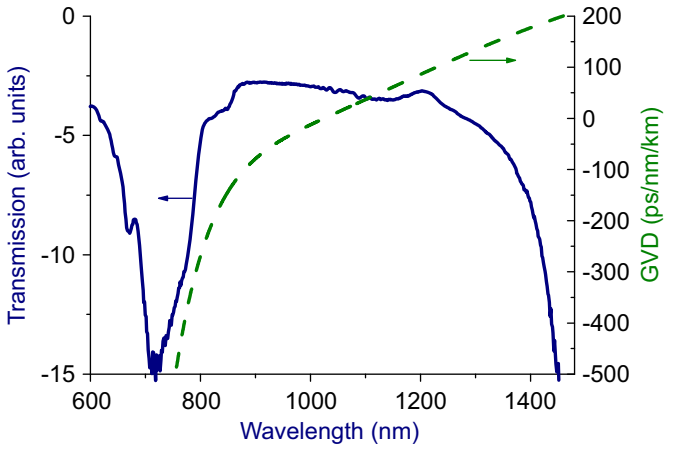

Fig. 2. Transmission spectrum (solid line) and the profile of group-velocity dispersion (dashed line) of the all-solid photonic band-gap fiber with the cross-section structure as shown in inset 1. An image of the 1040 nm laser beam transmitted through the all-solid PBGF is presented in inset 2.

system into sub-100 fs, 6.4 nJ light pulses smoothly tunable within the range of wavelengths from 1160–1260 nm.

The laser-oscillator and amplifier stages of the wavelength-tunable light source developed in this work employ diode-pumped ytterbium-doped single-polarization LMA PCFs (Fig. 3) in a stretcher-free configuration [8], delivering laser pulses with a central wavelength of 1040 nm and a maximum average power of 28 W at a pulse repetition rate of 50 MHz. An amplified LMA PCF laser output compressed to a 20 W, 100 fs pulse with a grating compressor was launched into a homemade all-solid non-polarization-maintaining PCF with a cross-section structure as shown in Fig. 1a and b. A silica cladding of this fiber includes a hexagonal periodic array of germanium-doped strands with a refractive index of 1.48 at 1040 nm running along the fiber. The diameter of each Ge-doped inclusion in the fiber cladding is 2 μm, with the pitch of the hexagonal lattice formed by these inclusions being 6 μm. The light is guided along a silica core in this fiber due to antiresonance reflection from the periodic structure of the cladding. The effective area of the fundamental mode of this fiber (Fig. 1c) is estimated as 110 μm^2 at a wavelength of 1040 nm.

The fiber is designed in such a way as to provide a broad transmission band around the central wavelength of our Yb-doped LMA PCF laser (Fig. 2) and to support a broadband wavelength tunability of solitons generated by the LMA PCF laser output. Spectrally resolved transmission measurements were performed by butt-coupling supercontinuum radiation from a highly nonlinear PCF into a 1 m section of the all-solid PBGF. The first transmission band of our all-solid PBGF stretches from 780 to 1400 nm (Fig. 2). Spatially resolved measurements, performed by imaging a low-intensity 1040 nm LMA PCF laser beam transmitted through the fiber on a CCD camera (inset 2 to Fig. 1), confirm that more than 95% of laser energy at the fiber output is concentrated in the fundamental mode of the fiber. This result is confirmed by M^2 measurements performed on the beam at the fiber output. According to the measurements and finite-element analysis, the group-velocity dispersion (GVD) of the fundamental mode of the PBGF is anomalous everywhere within the first transmission band for wavelengths longer than 1060 nm (the dashed line in Fig. 2).

Fig. 4a shows a map of the spectrally resolved PBGF output measured as a function of the average power of input 100 fs LMA PCF laser pulses with a spectrum as shown by the dashed line in Fig. 5. The central wavelength of input radiation falls within the range of normal fiber dispersion. As a result, for input average powers below 0.9 W, no soliton formation is observed in the PBGF output. The spectral transformation of the LMA PCF pulses in this regime is dominated by self-phase modulation (SPM). For higher input powers (above 1 W in Fig. 4a), SPM-induced spectral broadening starts to generate sufficiently intense spectral content in the region of anomalous fiber dispersion, giving rise to soliton formation. These solitons experience soliton self-frequency shift due to the Raman effect [19], leading to the generation of an intense redshifted component in the PBGF output. As can be seen from Figs. 4a and 6, the central wavelength of this component can be tuned from 1160 to 1260 nm by increasing the input laser power from 1 to 2.4 W. For higher input powers, the central wavelength of the frequency-shifted soliton PBGF output fell outside the transmission band of the fiber, leading to a substantial reduction in the soliton output power.

The above-outlined scenario of laser-pulse dynamics in the all-solid PBGF is verified by numerical modeling based on the standard nonlinear Schrödinger equation (NLSE) [19]. This modeling, as can be seen from Figs. 4a, 4b, and 5, reproduces the main tendencies in the dynamics of solitons excited by laser pulses in the all-solid PBGF used in our experiments. Specifically, the wavelength shift of the soliton PBGF output calculated as a function of the average power injected in the fiber at a central wavelength of 1070 nm (i.e., around the high-frequency edge of the anomalous dispersion region) closely follows the soliton redshift in the experimental map. NLSE-based simulations, as can be seen from Fig. 4a and b, accurately reproduce the tunability range of the soliton fiber output achieved in experiments (1160 to 1260 nm) and provide an adequate fit for the spectra of the soliton PBGF output (Fig. 5).

With an appropriate spectral filter applied to select the wavelength-shifted soliton from the nonsolitonic part of the field at the output of the PBGF, the maximum average power of the soliton with a central wavelength of 1260 nm was estimated as

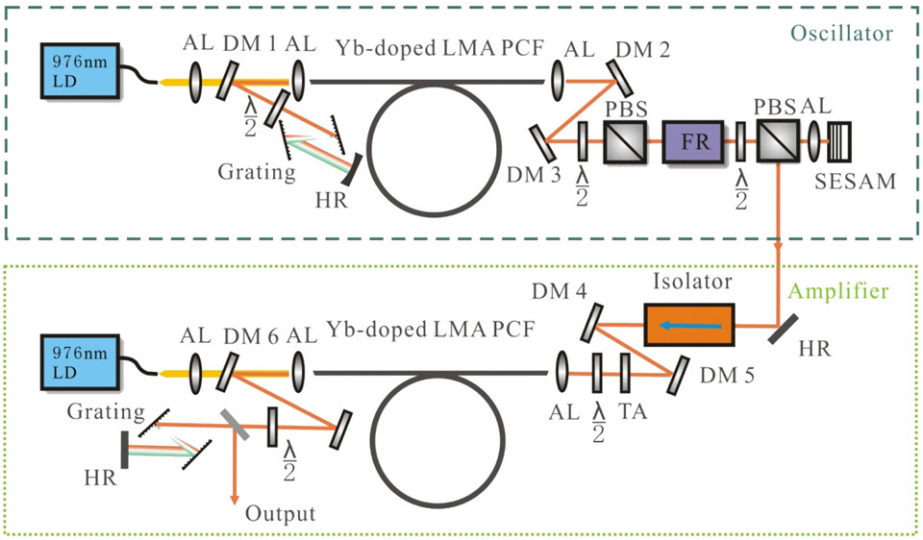

Fig. 3. Diagram of the Yb LMA PCF laser oscillator–amplifier system: LMA PCF, large-mode area photonic-crystal fiber; LD, laser diode; SESAM, semiconductor saturable-absorber mirror; FR, Faraday rotator; PBS, polarization beam splitter; AL, aspheric lens; DM, dichroic mirror; HR, high-reflectivity mirror.

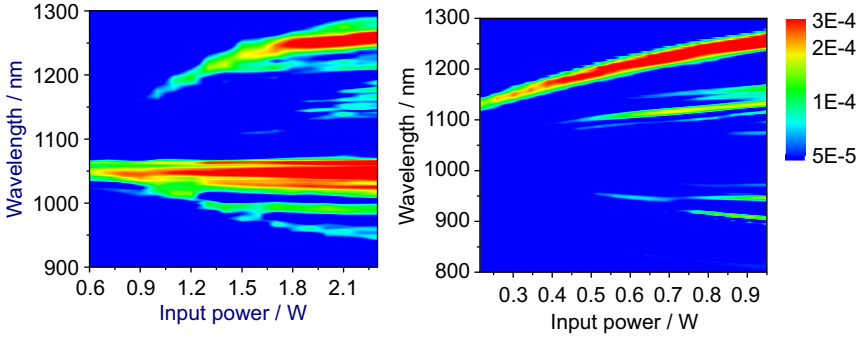

Fig. 4. (a) Spectrally resolved PBGF output measured as a function of the average power of input 100 fs 50 MHz LMA PCF laser pulses. The fiber length is 30 cm. (b) Spectrally resolved PBGF output calculated as a function of the average power injected in the fiber at a central wavelength of 1070 nm.

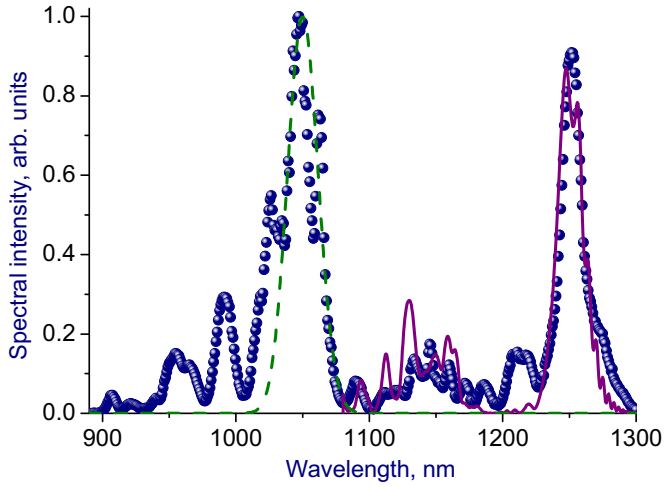

Fig. 5. Measured (circles) and simulated (solid line) spectra of the PBGF output. The input spectrum is shown by the dashed line. The input laser power in experiments is 2.4 W. The fiber length is 30 cm.

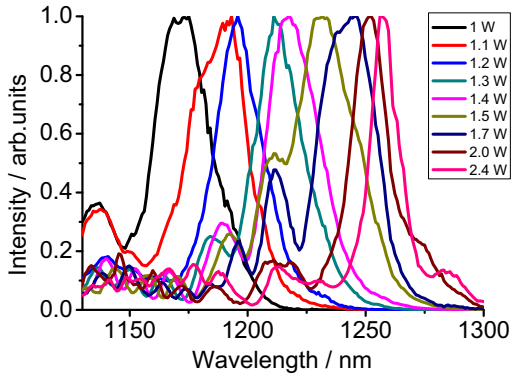

Fig. 6. Spectra of the solitons generated at the output of the all-solid PBGF with different average powers of input LMA PCF laser pulses.

320 mW, which corresponds to an energy of 6.4 nJ. The pulse width of this soliton was measured with the use of the auto-correlation technique. The measured autocorrelation trace of the soliton PBGF output (circles in Fig. 7) only slightly deviates in its edges from an autocorrelation trace calculated for an ideal hyperbolic-secant-shaped soliton pulse with a pulse width of 84 fs (dashed line in Fig. 7). This estimate for the soliton pulse width agrees well with the results of numerical simulations, predicting a pulse width of 82 fs for a frequency-shifted soliton with a central wavelength of 1260 nm (the inset in Fig. 7).

In conclusion, we have demonstrated a wavelength-tunable source of high-energy sub-100 fs light pulses where all the key components, including a master oscillator, an amplifier, and a

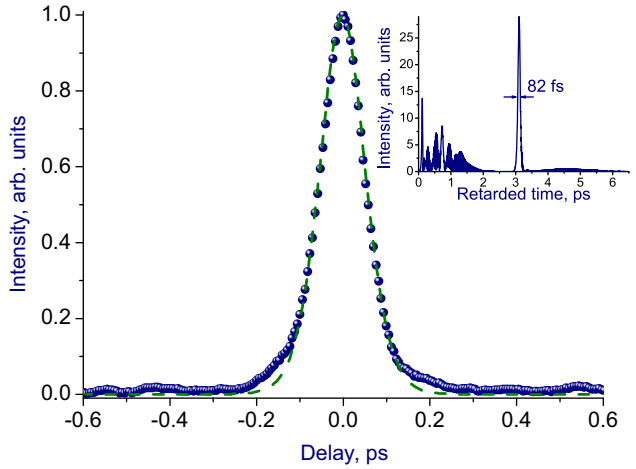

Fig. 7. Autocorrelation trace of the spectrally filtered PBGF soliton output with a central wavelength of 1260 nm (filled circles) and a hyperbolic-secant-shaped pulse with a pulse width of 84 fs (dashed line). The inset shows the results of NLSE-based simulations for the spectrally filtered 1260 nm soliton at the output of the PBGF under the same conditions.

tunable frequency shifter, are based on photonic-crystal fibers. Wavelength-tunable solitons along with the residual 1040 nm nonshifted component represent a typical two-frequency output of an all-solid PBGF in our experiments, which offers much promise for two-color spectroscopy, microscopy, and imaging techniques, including high-resolution two-photon microscopy, chemically selective microspectroscopy of coherent anti-Stokes Raman scattering, multicolor neuroimaging, and two-color time-resolved pump-probed studies.

Acknowledgments

This work was supported in part by the National Basic Research Program of China (Grant nos. 2011CB808101 and 2010CB327604), National Natural Science Foundation of China (Grant nos. 60838004 and 61078028), the Foundation for the Author of National Excellent Doctoral Dissertation (Grant no. 2007B34), the Russian Foundation for Basic Research, the Welch Foundation (grant no. A-1801), the Skolkovo Foundation (grant no. 78), and the High-end Foreign Experts Program (GDW-20121200044).

References

[1] P.St.J. Russell, Science 299 (2003) 358.
[2] J.C. Knight, T.A. Birks, R.F. Cregan, P.St.J. Russel, J.-P. de Sandro, Electronics Letters 34 (1998) 1347.
[3] K. Furusawa, A. Malinowski, J. Price, T. Monro, J. Sahu, J. Nilsson, D. Richardson, Optics Express 9 (2001) 714.
[4] J. Limpert, F. Röser, T. Schreiber, A. Tünnermann, IEEE Journal of Selected Topics in Quantum Electronics 12 (2006) 233.
[5] F. Röser, T. Eidam, J. Rothhardt, O. Schmidt, D.N. Schimpf, J. Limpert, A. Tünnermann, Optics Letters 32 (2007) 3495.
[6] Y. Zaouter, D.N. Papadopoulos, M. Hanna, J. Boullet, L. Huang, C. Aguergaray, F. Druon, E. Mottay, P. Georges, E. Cormier, Optics Letters 33 (2008) 107.
[7] F. Röser, J. Rothhard, B. Ortac, A. Liem, O. Schmidt, T. Schreiber, J. Limpert, A. Tünnermann, Optics Letters 30 (2005) 2754.
[8] B.W. Liu, M.L. Hu, X.H. Fang, Y.Z. Wu, Y.J. Song, L. Chai, C.Y. Wang, A.M. Zheltikov, Laser Physics Letters 6 (2009) 44.
[9] A.V. Mitrofanov, A.A. Ivanov, M.V. Alfimov, A.A. Podshivalov, A.M. Zheltikov, Optics Communications 280 (2007) 453.
[10] A.B. Fedotov, A.A. Voronin, I.V. Fedotov, A.A. Ivanov, A.M. Zheltikov, Optics Letters 34 (2009) 851.
[11] T. Südmeyer, F. Brunner, E. Innerhofer, R. Paschotta, K. Furusawa, J.C. Baggett, T.M. Monro, D.J. Richardson, U. Keller, Optics Letters 28 (2003) 1951.
[12] T. Eidam, F. Roser, O. Schmidt, J. Limpert, A. Tunnermann, Applied Physics B 92 (2008) 9.
[13] I. Martial, D. Papadopulos, M. Hanna, F. Druon, P. Georges, Optics Express 17 (2009) 11155.
[14] F. Luan, A.K. George, T.D. Hedley, G.J. Pearce, D.M. Bird, J.C. Knight, P.St.J. Russell, Optics Letters 29 (2004) 2369.
[15] A. Isomäki, O.G. Okhotnikov, Optics Express 14 (2006) 9238.
[16] B. Kibler, T. Martynkien, M. Szpulak, C. Finot, J. Fatome, J. Wojcik, W. Urbanczyk, S. Wabnitz, Optics Express 17 (2009) 10393.
[17] A. Bétourné, A. Kudlinski, G. Bouwmans, O. Vanvincq, A. Mussot, Y. Quiquempois, Optics Letters 34 (2009) 3083.
[18] I.V. Fedotov, A.A. Lanin, A.A. Voronin, A.B. Fedotov, A.M. Zheltikov, O.N. Egorova, S.L. Semjonov, A.D. Pryamikov, E.M. Dianov, Journal of Modern Optics 57 (2010) 1870.
[19] G.P. Agrawal, Nonlinear Fiber Optics, 4th edition, Academic, San Diego, 2007.